Atmospheric Environment 147 (2016) 330–343

Contents lists available at ScienceDirect

Atmospheric Environment

journal homepage: www.elsevier.com/locate/atmosenv

Development of a baseline-temperature correction methodology for electrochemical sensors and its implications for long-term stability

Olalekan A.M. Popoola*, Gregor B. Stewart, Mohammed I. Mead, Roderic L. Jones

Department of Chemistry, University of Cambridge, Cambridgeshire, UK

HIGHLIGHTS

- Temperature correction of low cost air quality sensors.
- Developed a robust baseline-temperature correction methodology.
- Methodology shown to be reproducible for different gas species.
- Temperature corrected data show good agreement with reference instrument.
- Long term gain/sensitivity of sensors not affected by meteorology.

ARTICLE INFO

Article history:
Received 16 May 2016
Received in revised form
10 October 2016
Accepted 14 October 2016
Available online 14 October 2016

Keywords:
Air quality
Electrochemical sensors
Long-term measurements
Nitric oxide
Carbon monoxide
Baseline-temperature correction

ABSTRACT

Recent studies have shown that (three-electrode) electrochemical sensors can be utilised for air quality monitoring and exposure assessment. The long-term performance of these sensors is however, often limited by the effects of ambient meteorological parameters on the sensor baseline, in particular temperature. If electrochemical (EC) sensors are to be adopted for air quality measurement over extended periods (months), this effect must be accounted for. Recent long-term, ambient measurements of CO, NO and NO_2 using EC sensors have revealed that temperature (and relative humidity (RH)) had an effect on the baseline which was more pronounced in the case of NO sensors with coefficient of determination, R^2 of 0.9 when compared to CO and NO_2 with $R^2 < 0.2$. In this paper we present a correction methodology that quantifies this effect (referred to here as fitted baseline), implementing these correction on the EC measurements. We found that EC sensors corrected for baseline-temperature effect using the method describe in this paper show good agreement when compared with traditional reference instrument. The coefficient of determination R^2 of 0.7–0.8 and gradient of 0.9 was observed for baseline-temperature corrected NO compared to $R^2 = 0.02$ prior to baseline-temperature correction. Furthermore, the correction methodology was validated by comparing the temperature-baseline with proxy temperature compensating measurements obtained from the fourth electrode of a set of novel four-electrode electrochemical sensors. A good agreement ($R^2 = 0.9$, with gradients = 0.7–1.08 for NO and $0.5 < R^2 < 0.73$ for CO) was observed between temperature fitted baselines and outputs from the fourth electrodes (also known non-sensing/auxiliary electrode). Meanwhile, the long-term stability (calibrated signal output) of temperature-corrected data was evaluated by comparing the change in sensor gain to meteorological parameters including temperature, relative humidity, wind speed and wind direction. The results showed that there was no statistically significant change in sensitivity (two-sided *t*-test, $p = 0.34$) of the temperature-corrected electrochemical sensor with respect to these parameters (over several months). This work demonstrates that using the baseline-temperature correction methodology described in this paper, electrochemical sensors can be used for long-term (months), quantitative measurements of air quality gases at the parts per billion volume (ppb) mixing ratio level typical of ambient conditions in the urban environment.

© 2016 The Authors. Published by Elsevier Ltd. This is an open access article under the CC BY license (http://creativecommons.org/licenses/by/4.0/).

Abbreviations: EC, electrochemical; WE, working electrode; AE, the auxiliary electrode; LAQN, Local Air Quality Network; SNAQ-Heathrow, sensor networks for air quality at London Heathrow airport; CCC, Cambridge City Council; DTG, Digital Technology Group; AURN, the UK Automatic Urban and Rural Network; CHL, chemiluminescence analyser.

* Corresponding author.
E-mail address: oamp2@cam.ac.uk (O.A.M. Popoola).

http://dx.doi.org/10.1016/j.atmosenv.2016.10.024
1352-2310/© 2016 The Authors. Published by Elsevier Ltd. This is an open access article under the CC BY license (http://creativecommons.org/licenses/by/4.0/).

1. Introduction

Health effect of air quality gases such as carbon monoxide (CO), nitric oxide (NO) and nitrogen dioxide (NO_2) is well documented. As part of the European Union (EU) air quality directive, member nations are required to monitor air quality gases in area where levels are predicted to exceed limits set by the body (EU directives 1998, 2009). Routine monitoring are carried out using reference technique which are based on established techniques such as chemiluminescence used for NO, NO_2 monitoring and dispersive infra-red for CO. While these techniques have been shown to be highly sensitive with high temporal resolution, they are very expensive to install and run, requiring routine maintenance, and highly secured locations. This limits the number of monitoring stations that can be setup, thereby limiting spatial air quality data coverage.

Air quality is highly heterogeneous in space, to better understand the chemistry and exposure studies it is important to have good spatial information on air pollutants. Recent work has shown application of low-cost electrochemical sensor nodes in air quality network studies (Mead et al., 2013; De Vito et al., 2009). These sensor nodes measure CO, NO and NO_2 in addition to ambient temperature. While using short term studies (hours) have demonstrated the reliability of these sensor nodes in capturing temporal and spatial variability in air quality, long term (days to weeks) deployments for air quality assessment have proven to be much more challenging. Measurements from the latter are affected by the diel variations in ambient temperatures which affect the baselines of the measured pollutant a situation which is not experienced in the former. Although sensor manufactures tend to provide temperature/RH dependent data (Alphasense, AAN), these are however not sufficient enough to account for the additional problems encountered in operating these sensors in real world (see details in Section 3.5). In order to utilise electrochemical sensor nodes as indicative techniques for air quality assessment, it becomes imperative to develop a baseline-temperature correction methodology to account for the change in baseline resulting from variations in ambient temperature.

The work presented in this paper explains the methodology developed to address this problem through quantitative extraction and correction of temperature-dependent baseline effects.

1.1. Electrochemical sensors

Most of the works presented in this paper are based on the use of three-electrode electrochemical sensors. The four electrode electrochemical sensors are only included in this work to validate the baseline correction methodology.

1.1.1. Three-electrode electrochemical sensors

The main electrochemical sensor nodes used in this work utilise CO-AF, NO-A1 and NO_2 A1 electrochemical sensors manufactured by Alphasense Ltd, UK. They are made of three electrodes: working (sensing electrode), counter electrode and reference electrode. These electrodes are in contact with an electrolyte made of highly concentrated sulphuric acid via a wetting filter. As with all electrochemical cells, current is generated by the flow of electrons resulting from the reduction-oxidation (redox) reaction occurring at the electrode-electrolyte interphase. Oxidation/reduction half reaction of the target gas occurs at the working electrode (WE), while the counter electrode completes the redox reaction by reducing oxygen or oxidising water molecules. Electrochemical reactions are governed by Nernst equation which relates the natural logarithm of the ratio of the activities of the oxidant and reductant to temperature, number of moles of electrons involved in the reaction, temperature, Faradays constant and the cell potential. This type of electrochemical cell is referred to as potentiometric cell. However, if the active electrode is maintained at a constant voltage, then the electrochemical cell is said to be operated as an amperometric cell, in which case the current generated by the redox reaction is related to the concentration of the target gas (Stetter and Li, 2008). The reference electrode is used to anchor the WE at a stable potential, this is achieved by connecting it to the WE via a potentiostat (Fig. 1).

1.1.2. Four-electrode electrochemical sensors

More recently Alphasense have developed a novel four-electrode electrochemical sensor which were used in a recent project involving the deployment of sensor networks for air quality at London Heathrow airport (SNAQ-Heathrow project) (Popoola et al., 2013). The additional electrode in this new sensor called the auxiliary electrode (AE) is similar in design material as well as arrangement to the WE. However, the AE is not in contact with the target gas. It therefore provides useful information on the effect of ambient condition mostly temperature on the output of WE. In this work, raw EC data refer to the mixing ratio equivalents of the currents recorded at WE while AE outputs are mixing ratio equivalents of baseline-temperature dependence of WE. As part of the validation section for the baseline-temperature correction method, the fitted baseline presented in this work will be compared to AE outputs. The particular sensors used in the work presented here were the CO-B4 and NO-B4 sensor from Alphasense.

1.2. Electrochemical sensor nodes

Details of the mobile electrochemical sensor nodes used in this work have been reported (Mead et al., 2013). In summary, each sensor node is made up of three-electrode electrochemical sensor measuring CO, NO and NO_2. Each node also has temperature sensor as well as GPS and GPRS module for position/time and data transmission. The temporal resolution of the data is 5 s and all sensor nodes are powered by main power supply throughout the duration of the deployment.

1.3. Fundamental temperature effects on electrochemical sensors

The electrochemical sensors used in this study are designed to work as amperometric devices, configured in such that the output current is limited by the diffusion of gases into the sensor (Mead et al., 2013). In this mode of operation, the overall current is the summation of the current that results from diffusion across four regions, namely: the electrolyte–electrode, membrane, gas space

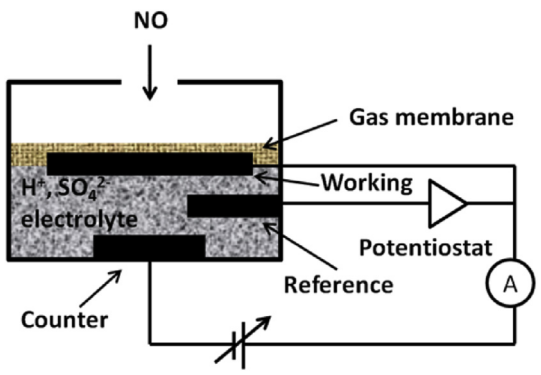

Fig. 1. Schematic of an amperometric NO electrochemical gas sensors showing the basic components including three electrodes, electrolyte and gas membrane.

and sensor aperture, as shown in Fig. 2.

For each region, the diffusion flux j across the barrier can be expressed in terms of Fick's first law, as follows:

$$j = -D\frac{\Delta C}{\Delta y} \quad (1)$$

where D is the diffusion constant, ΔC is the difference in the mixing ratio of the diffusing species at the edges of the barrier and Δy is the distance across the barrier in the y direction (this can be a, b, l or w, as shown in Fig. 1). The negative sign of Eq. (1) indicates that flow is in the opposite to the direction of y. If we consider the diffusion across the electrolyte to the electrode surface, then Eq. (1) can be written as:

$$j_e = -D_e\frac{C_{e,o}}{a} \quad (2)$$

where D_e is the diffusion coefficient, $C_{e,o}$ is the difference in the mixing ratio of the diffusing species at the edges between the electrolyte and the electrode and a is the distance between the electrolyte and the electrode surface. The total current (I_e) generated by the sensor across the electrolyte-electrode interface is related to the j_e by the expression $I_e = nFA_ej_e$, where n is the number of electrons involved in the redox reaction, F is Faraday's constant and A_e is the area of the electrocatalyst (Hitchman et al., 1997). After substituting j_e using the expression in Eq. (2), I_e can be represented the following expression (Eq. (3)):

$$I_e = -\frac{nFA_eD_eC_{e,o}}{a} \quad (3)$$

The total current I_h, I_m and I_g can also be written for the diffusion across the hole, membrane and gas space respectively. These currents have diffusion constants D_h, D_m and D_g respectively. The diffusion coefficient, D_m, can be Fickian, Knudsen or surface diffusion coefficient depending on the type of diffusion taking place across the barrier while D_h and D_g are Fickian diffusion coefficient (Hitchman et al., 1997). The overall sensor current (I) resulting from diffusion across the different barriers is represented by Eqn. (4).

$$\frac{1}{I} = \frac{1}{I_e} + \frac{1}{I_m} + \frac{1}{I_g} + \frac{1}{I_h} \quad (4)$$

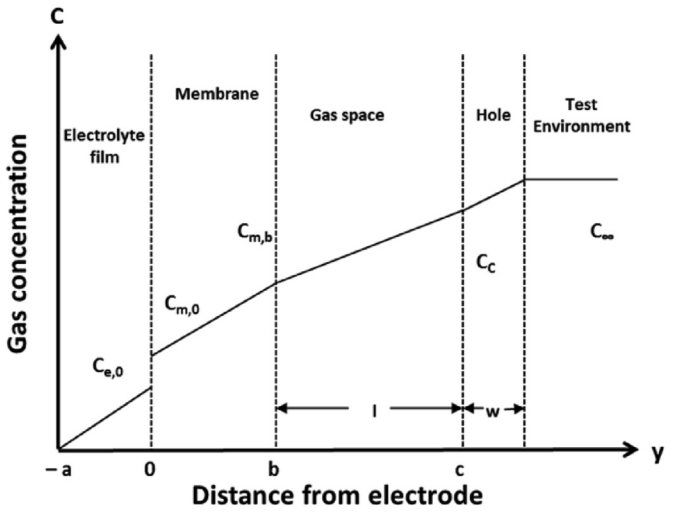

Fig. 2. Diffusion barriers and concentration for a membrane-covered electrochemical sensor. Modified after Hitchman et al., 1997.

Studies have shown that, for Fickian diffusion, the current is proportional to square root of temperature in Kelvin ($I \propto T^{1/2}$), whereas I is proportional to $T^{-1/2}$ for Knudsen diffusion (Hitchman et al., 1997). An exponential dependence of I (a measure of the dissolved gas mixing ratio) to temperature has also been reported (Hitchman, 1978). If one considers the complex interactions across the various barriers and non-idealised practical applications, we observe in fact a single function relating temperature to the current does not adequately define this relationship and that other environmental factors or sensor drift can influence the observed outputs. As a result an additional correction methodology has to be developed for the electrochemical sensor nodes described in this paper.

2. Determination and correction of temperature-baseline effect

2.1. Study areas

The data presented in this paper were collected from two air quality monitoring stations located within the city centre in Cambridge, UK. These sites are designated site 1 and site 2 in this paper. Although the main results presented in this paper are from site 1, results from site 2 aids in demonstrating the need for the correction methodology described in this paper. At both locations, electrochemical sensor nodes measuring CO, NO and NO_2 as well as temperature were deployed. In addition to measurements from the sensor nodes, NO and NO_2 measurements from reference instruments operated by the Environmental Department of the Cambridge City Council (CCC) are presented in this paper.

Local meteorological variables including RH, wind speed and direction for the duration of the deployment were obtained from the Digital Technology Group (DTG) Weather Station located at the Computer Laboratory, University of Cambridge (N 52°12′39.27″ E 0°5′32.01″).

Site 1 is situated close to a busy junction linking four major roads (Gonville Place, Hills Road, Regent Street and Lensfield Road), as shown in Fig. 3. It is part of the Local Air Quality Network (LAQN) and is referred to as the Gonville Place LAQN station. In contrast, site 2 is situated on Regent Street, which is a major route to and from the bus station located in the Cambridge city centre (Fig. 3). This monitoring station has been designated a roadside station by the Cambridge City Council (CCC) Environmental Department and is part of the UK Automatic Urban and Rural Network (AURN). The most significant meteorological factor that differed between these sites was temperature. The comparison of data between both sites provided an excellent opportunity to investigate how ambient temperature variation affects the performance of electrochemical based air quality sensors.

At site 2, air is drawn in through a co-located inlet at a height of 4 m (inset Fig. 3) and feeds into the two different instrumentations - pair of electrochemical sensor nodes and chemiluminescence instrument (described in section 2.2) which are located indoors. The ambient temperature at site 2 is well controlled (room temperature) and hence this site provides an excellent opportunity to validate if ambient temperature has any influence on the long term measurements from electrochemical sensors. In contrast, the electrochemical sensors located at site 1 (left panel Fig. 3) were exposed to the large variations in ambient daily temperature. Hence if the electrochemical sensors respond to diel variations in temperature this will be a good location to test the effect.

2.2. Instrumentations

A pair of electrochemical sensor node measuring CO, NO and

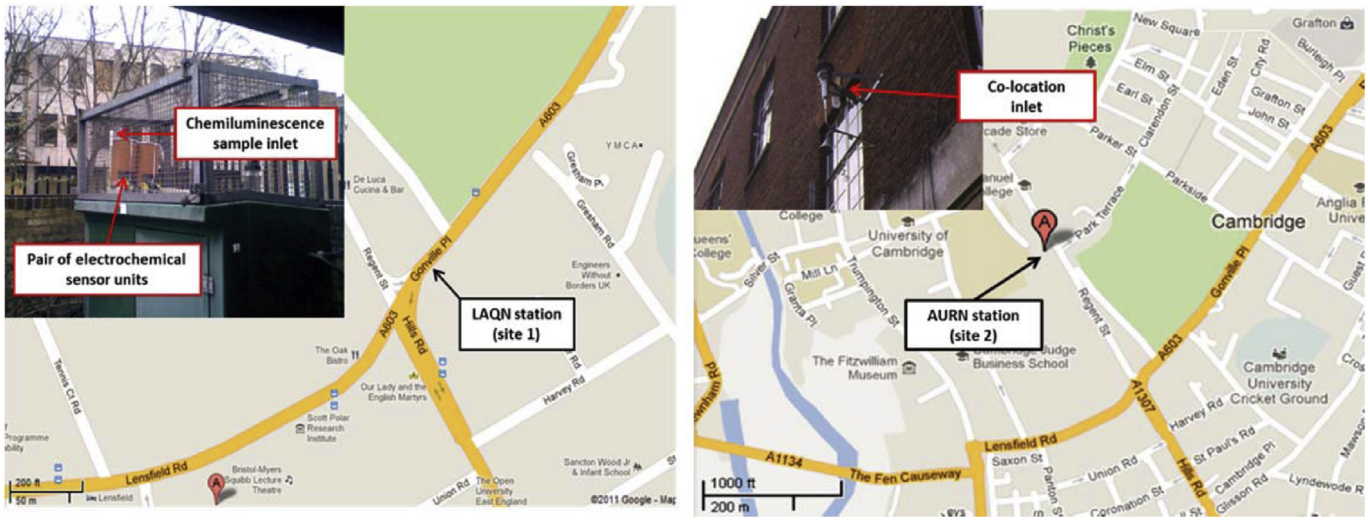

Fig. 3. Maps to show the location of the two test sites in Cambridge, UK. The left panel shows the LAQN station (site 1) at Gonville Place, Cambridge, UK. The inset photo shows the co-location of two electrochemical sensor instruments (housed in weather-proof enclosures) with the chemiluminescence unit at the LAQN station. The right panel shows the AURN monitoring station (site 2) in Regent Street, Cambridge, UK. The sampling inlet of the monitoring station located on the first floor of the Cambridge City Council Building is shown in the inset photo. Images courtesy of Cambridge City Council and map courtesy of Google Maps.

NO_2 as well as ambient temperature was used at the two study area described in Section 2.1. Although the basic configuration of the two pair of sensor nodes were similar, the NO_2 measurements from the pair deployed at site 1 were subject to large degrees of electronic noise (≈20 ppb) unlike the sensor nodes at site 2 (noise < 5 ppb) (Mead et al., 2013). In addition as shown in the Mead et al. paper, the NO_2 sensors are actually measuring the sum of NO_2 and O_3. As this work aims at presenting a method for baseline temperature correction rather accounting for cross sensitivity correction, only CO and NO data from EC1 and EC2 at site 1 were used in the baseline temperature correction. At both sites, ratified NO and NO_2 measurements were obtained from reference NO_X chemiluminescence instruments (DEFRA, 2009) (referred to hereafter as CHL) operated by CCC.

2.3. Data processing

The methodology presented in this work used mainly data from the two types of instrumentations (electrochemical sensor nodes and chemiluminescence instruments) are presented in this work. High temporal resolution (5 s measurements) data from the electrochemical sensor nodes were used in the baseline-correction methodology described in this paper. In contrast, data from the chemiluminescence instruments are reported as hourly mean averages and therefore for the validation of the baseline correction methodology, hourly mean average of the 5 s data from sensor nodes were used. Since the correction methodology described in this paper uses high temporal resolution measurements from the sensor nodes, NO_2 measurements from site 1 were excluded from the analysis presented here for reasons stated in Section 2.2. The rest of this paper will therefore focus on baseline-temperature correction of CO and NO data acquired using the electrochemical sensor nodes, with the assumption that this correction methodology can be used for similar electrochemical sensor nodes that also show temperature-baseline dependence. The macro meteorology data used in the stability analysis are also hourly mean averages. As

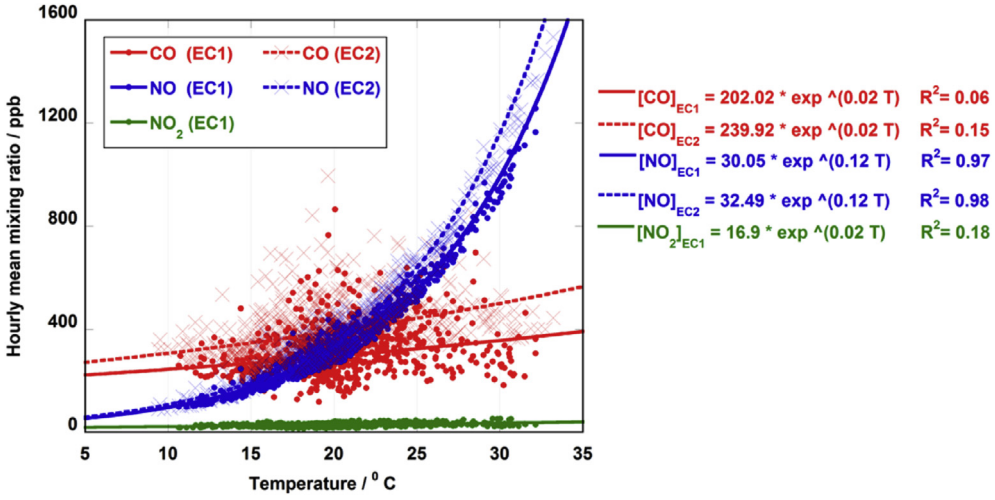

Fig. 4. Scatter plots showing the relationship between hourly mean CO, NO and NO_2 mixing ratios and temperature observed over a month-long period (2–28 September 2010) during the long-term deployment at the local air quality network (LAQN) station in Gonville Place, Cambridge (February–December 2010). Note the NO_2 measurements from EC2 failed during this deployment; hence no data was reported for this species.

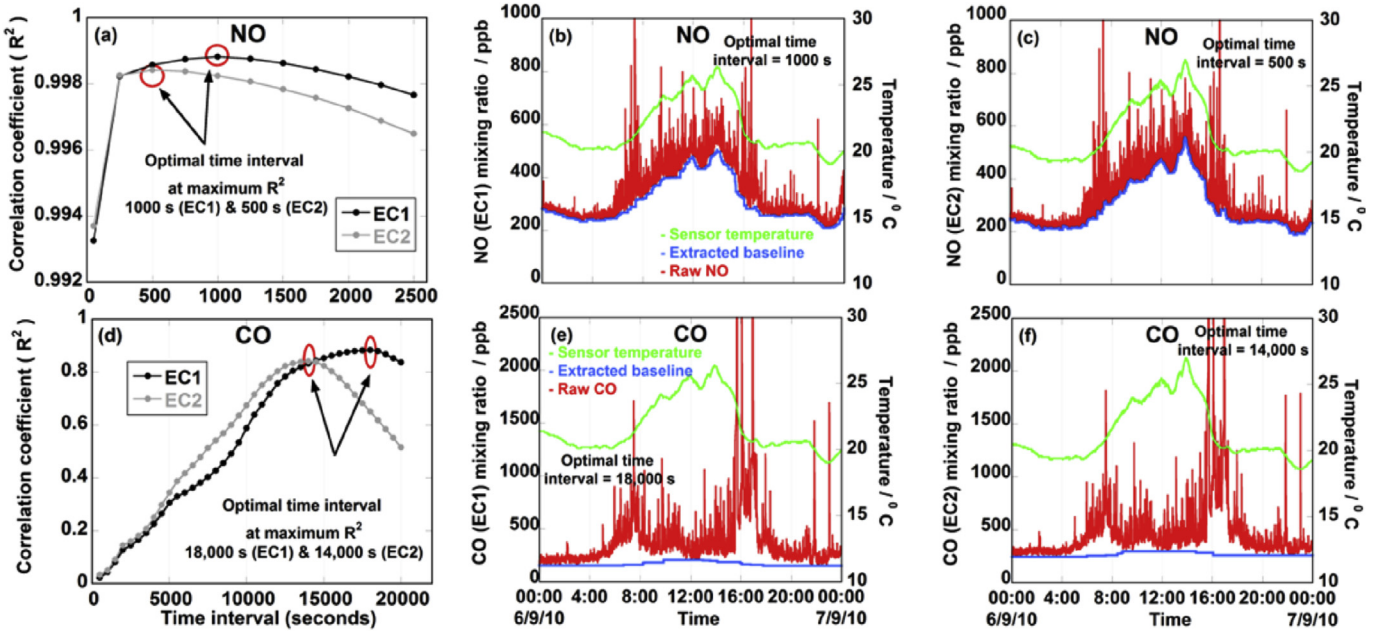

Fig. 5. An example plot showing varying time intervals against R^2 (a) and (d) and a time series of CO and NO mixing ratios (observed in EC1 and EC2) with temperature and extracted baselines derived from the optimal time interval over a 24-h period (b), (c), (e) and (f). Notice the optimum time window is the turning point of the points in (a) and (c), in this case 500 s (EC1) and 1000 s (EC2) intervals for NO and 18,000 s (EC1) and 14,000 s (EC2) for CO.

mentioned 1.1.2., novel four-electrode based nodes were also used to validate the methodology and these data were high resolution 20 s data details of the data processing available in the SNAQ Heathrow project (Popoola et al., 2013).

2.4. Effect of ambient temperature on electrochemical sensors

Baseline of the data from the electrochemical sensor nodes are defined in this paper as the contribution to the overall measurements resulting directly from the influence of ambient temperature excluding any contributions from regional and local traffic sources.

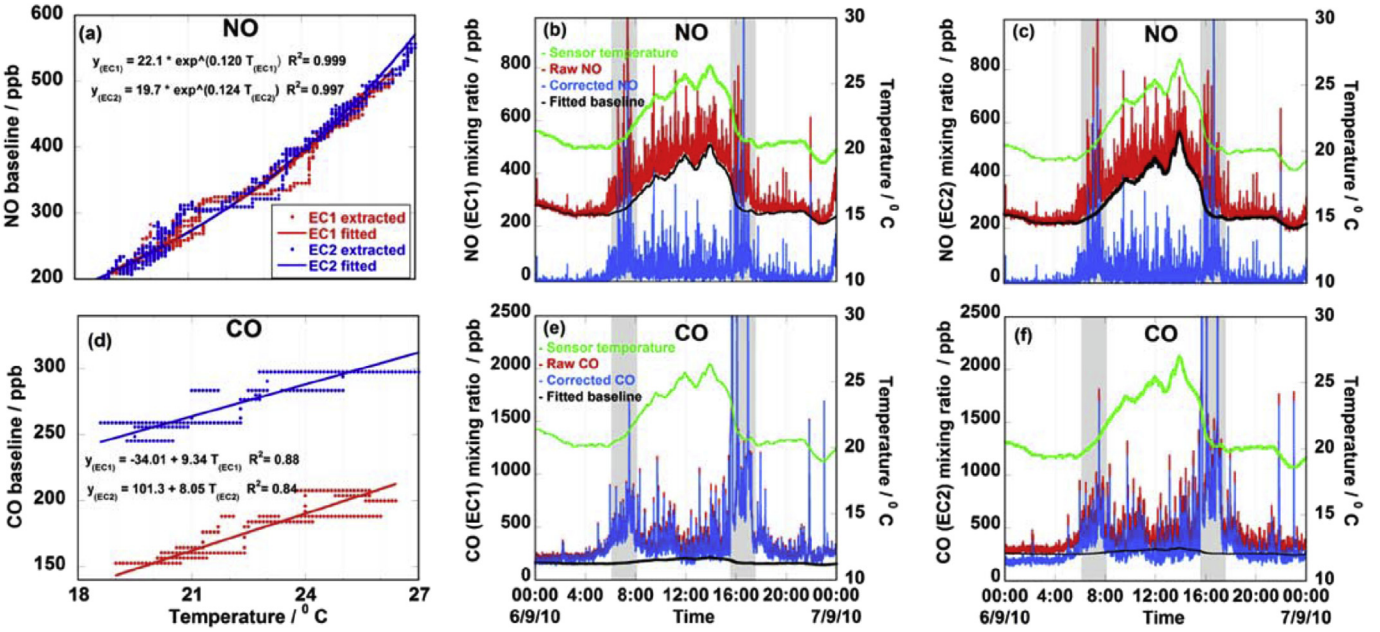

Fig. 6. A 24-h regression plot of temperature against temperature-dependent baseline changes (red represents that extracted and blue fitted) are shown in (a) and (d), whilst a time series of fitted baselines, temperature, raw NO and CO and corrected NO and CO mixing ratios for a typical 24-h period are presented in (b), (c), (e) and (f). Note the morning and evening rush-hour peaks (0600–0800 and 1530 to 1730 grey shades) previously indiscernible from uncorrected raw NO (red (b) and (c)) relative to background measurements can now be seen in the corrected NO (blue (b) and (c)). In contrast, these peak events are evident against the baseline in the CO measurements in both the raw (red (e) and (f)) and corrected CO data (blue (e) and (f)), showing that the CO measurements show small temperature-dependent baseline change. (For interpretation of the references to colour in this figure legend, the reader is referred to the web version of this article.)

Table 1
Summary of hourly mean temperature statistics for air quality stations at both city-centre sites in Cambridge.

Site	Temperature/°C			Period of study
	Max	Min	Range	
1: Gonville Place	36.0	0.0	36.0	09/02/10–16/12/10
2: Regent Street	24.0	23.3	0.7	23/01/09–29/01/09

Since the contribution of ambient temperature to baseline measurements of the electrochemical sensors was unknown, the relationship between measurements of hourly mean temperatures and CO, NO and NO_2 mixing ratios were used in the first instance as a proxy for the relationship between temperature and sensor output for the different gas species (Fig. 4). It was observed for both sensor nodes at site 1 that the ambient temperature had the greatest effect on measured NO when compared to CO or NO_2. The output of the NO sensors showed a strong (exponential) relationship with temperature, with $R^2 \approx 0.9$ compared to 0.06 (EC1) and 0.15 (EC2) for CO and 0.18 for NO_2 (Fig. 4).

2.5. Baseline temperature-correction methodology

2.5.1. Extracting temperature-dependent baseline

A mathematical approach was developed in order to extract the daily baseline change due to temperature using the high temporal resolution (5 s) measurements of CO and NO from EC1 and EC2 at site 1. This was achieved by determining the minimum measurement value within a given time interval ($t \pm \delta t$) for each measurement at time, t, for every 24 h of data (assuming the urban background mixing ratios around 2 ppb and 200 ppb for NO and CO respectively (Bright et al., 2011)). This extracted minimum for every 24 h period (referred to as the "extracted baseline") was then correlated with ambient temperature measurements using the best mathematical relationship which were found to be exponential fit (for NO) and linear fit (for CO). The regression coefficient (R^2) between the extracted baseline and corresponding ambient temperature measurements was then determined. This process was repeated for varying time intervals δt (between 50 and 2500 s for NO and 500–20,000 s for CO). A plot of R^2 values against corresponding time intervals was used to determine the optimal time interval which corresponds to the maximum (or turning point) of the curve as shown in Fig. 5 (a) and (d). This optimal time interval was then used to generate the extracted baseline for each 24-h period of the data, examples of which are shown in Fig. 5 (b), (c), (e) and (f).

2.5.2. Baseline-temperature correction

Once the extracted baseline is determined, the fitted baseline (also referred to as temperature-dependent baseline) was determined. This was done by correlating extracted baselines with ambient temperature measurements using exponential and linear functions for NO and CO respectively, as depicted in Fig. 6 (a) and (d). Using the fit parameters obtained (offsets and the baseline change per unit change in temperature (db/dT)), and the ambient temperature measurements, the temperature-dependent baselines (black lines) were generated as shown in Fig. 6 (b), (c), (e) and (f). These baselines were then subtracted from the raw CO and NO measurements, with the resulting outputs giving the baseline-temperature corrected data. This correction methodology was then repeated for each 24-h period of the complete dataset. The rationale for repeating the correction methodology in blocks of 24-h is that it is a long enough time interval to observe a diel cycle in temperature measurements yet remains short enough to give the best fit between the extracted baseline and temperature measurements.

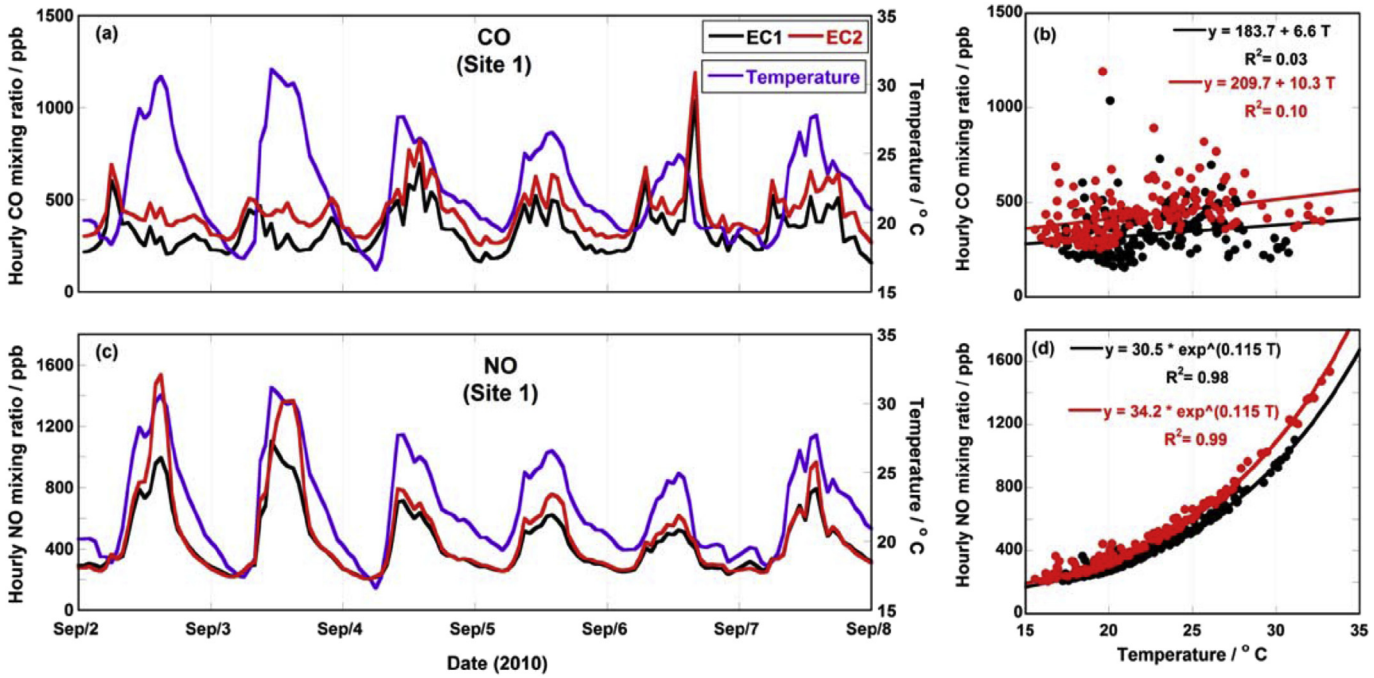

Fig. 7. Time series (a), (c) and regression plots (b), (d) of hourly mean CO and NO mixing ratios and temperatures for the ambient conditions at site 1, Gonville Place, Cambridge (2–8 September 2010).

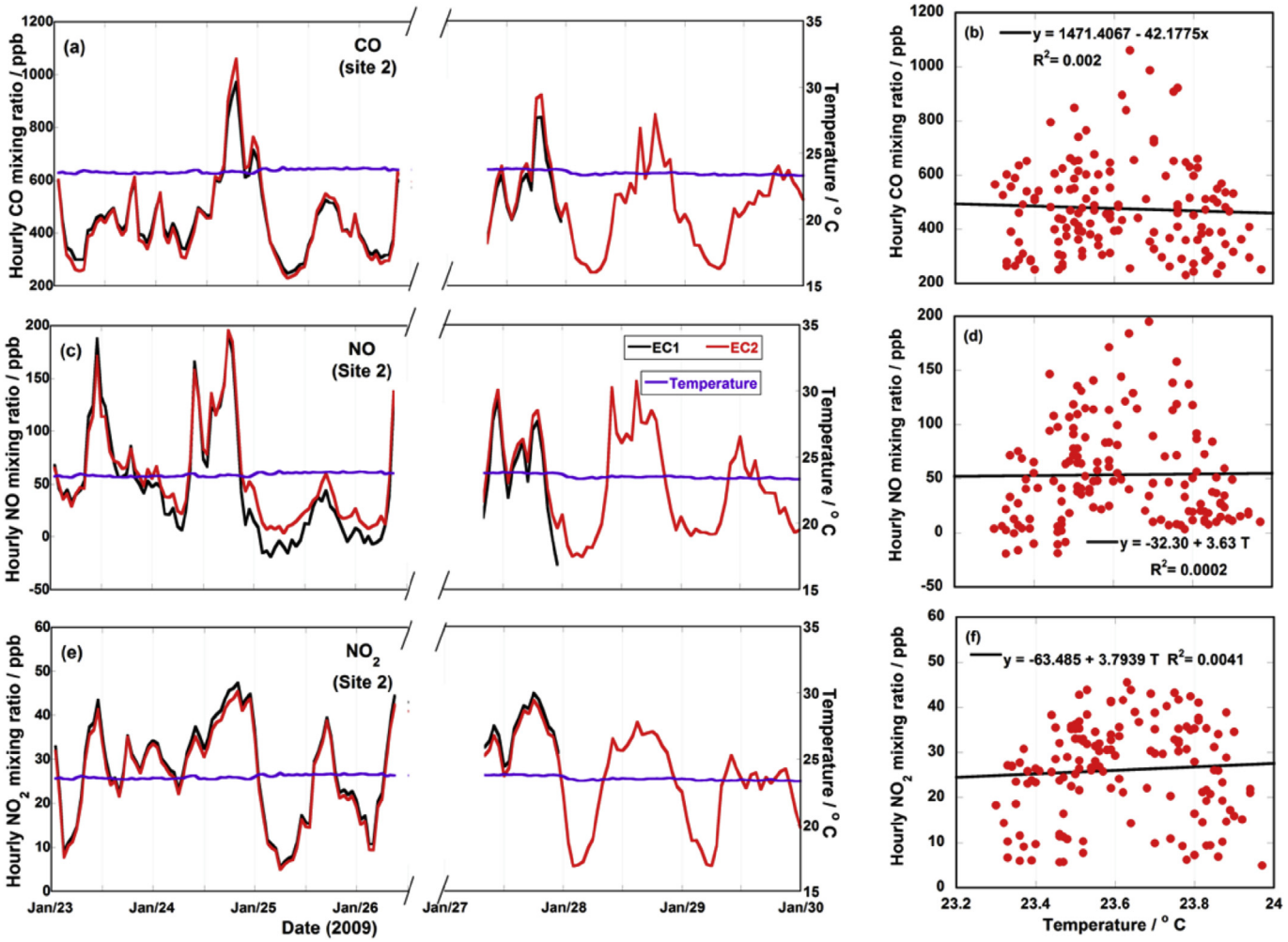

Fig. 8. Time series (a), (c), (e) and regression plots (b), (d), (f) of hourly mean CO, NO and NO_2 mixing ratios and temperatures for a controlled environment (indoor conditions) at the AURN site (site 2) in Regent Street, Cambridge (23–29 January 2009). Note the missing data in Fig. 8 is due to data transmission losses from the sensor nodes.

3. Results and discussion

3.1. Observed temperature effects on baseline measurements of electrochemical sensors

The hourly temperature ranges recorded for site 1 and site 2 are summarized in Table 1. Whilst temperatures ranged from 23.3 to 24.0 °C at site 2, range of 0.0–36.0 °C was observed at site 1 over the period of study. In addition, a diel variation in temperature was not observed at site 2 (Fig. 8), whilst the diel cycles are clearly visible in the measurements taken at site 1, as shown in Fig. 7. Figs. 4 and 6 indicate that the CO electrochemical sensors showed only a small baseline temperature dependence, in contrast to the NO electrochemical sensors, which showed a strong, exponential dependence with temperature for both long-term and short-term datasets, with an R^2 of 0.9 (Fig. 9).

In contrast, the results observed at site 2 showed that there was no visible relationship between CO, NO and NO_2 measurements with temperature, as depicted in Fig. 8 (b), (d) and (f). The variations seen in measurements at site 2 were due only to changing ambient CO, NO and NO_2 mixing ratios related mostly to road traffic sources. This is confirmed by the good agreement between the NO and NO_2 measurements of EC1 and EC2, and the CHL at this site (Fig. 10).

These results show that changing ambient temperature has a direct effect on the baseline of the signals of the electrochemical sensor nodes. Thus justifying the need for the correction presented in this paper.

3.2. Reproducibility of correction methodology

The reproducibility of this correction methodology was demonstrated by comparing results from baseline temperature corrected CO and NO data from the pair of electrochemical sensor nodes (EC1 & EC2) deployed at site 1. The time series and relationship plots for 5-s CO and NO measurements for one month during the deployment (2–28 September 2010) are shown in Fig. 11. A relationship coefficient of 0.92 was obtained between EC1 & EC2 for both species following the application of the baseline temperature-correction methodology, thus demonstrating the reproducibility of the correction technique. In addition, the mean mixing ratios over this period were within 3% of each other for EC1 and EC2, with values of 290 ppb and 300 ppb (CO), and 34 ppb and 35 ppb (NO) for EC1 and EC2 respectively. The summary of the statistics for temperature corrected CO and NO measurements from both electrochemical sensor nodes are shown in Table 2.

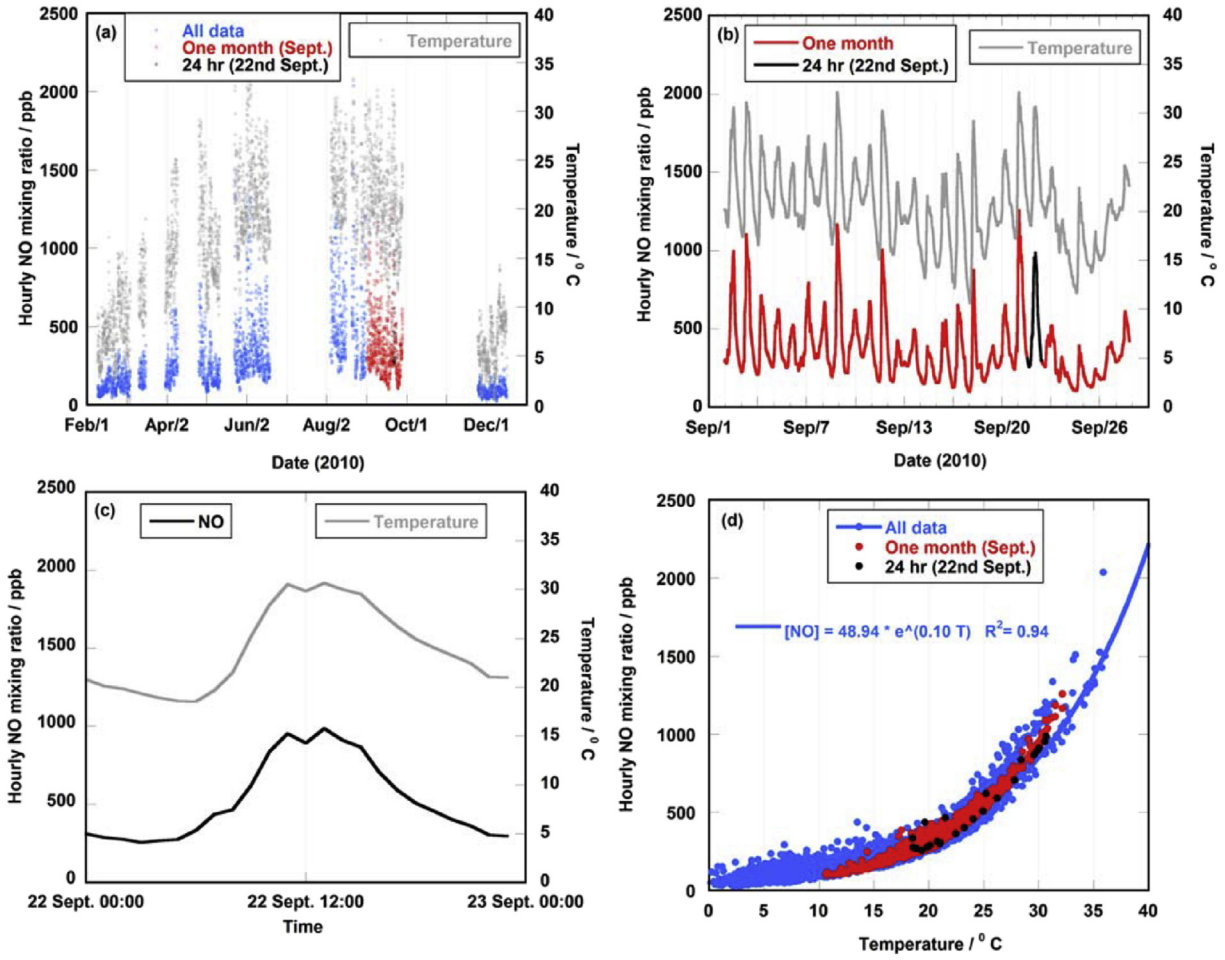

Fig. 9. Hourly mean temperature and measured NO mixing ratios using electrochemical sensor nodes at Gonville Place, Cambridge (site 1) for (a) the duration of the deployment (February–December 2010), (b) a one-month period during the deployment (2–28, September 2010) and (c) a 24-h period during the deployment (22 September 2010). A regression plot of hourly mean temperature and measured NO mixing ratios using electrochemical sensors, colour-coded based on length of data set, is shown in (d). The missing data in (a) correspond to periods over which the sensor nodes were not deployed.

3.3. Validation of correction methodology

The baseline correction methodology was validated in two ways. One method involves comparing the hourly mean baseline-temperature corrected EC data against hourly mean data from reference instrument. The other approach involves comparison of fitted baselines with auxiliary electrode 2 data of four-electrode EC sensors.

3.3.1. Statistical comparison of electrochemical sensor measurements with a reference (chemiluminescence) instrument

The correction methodology was validated by comparing hourly mean NO mixing ratios (measured using the electrochemical sensors), before and after temperature correction, with those measured using the chemiluminescence analyser (CHL) at the LAQN station at Gonville Place (site 1). There were no routine CO measurements made at this site and, as a result, CO could not be included in this comparison and for those reasons stated in Section 2.1, NO_2 measurements from the electrochemical sensors were also excluded from this analysis for reasons stated in Section 2.3. Although the NO measurements obtained from the pair of electrochemical sensor nodes have a temporal resolution of 5 s, for comparison, these data were averaged to give hourly means as the ratified data from the CHL are reported as mean hourly measurements. A summary of the relationship coefficients between NO measurements between the CHL and corrected as well as uncorrected NO from EC1 and EC2 is presented in Table 3.

As expected, there were poor relationship between the CHL and the pair of EC1 and EC2 for the uncorrected NO data, with $R^2 = 0.02$ (for both EC1 and EC2) for the complete dataset. However, after implementing the temperature correction, the agreement between the two instruments was significantly better. This improved agreement is also evident in the time series of the two different instruments (Fig. 12), with $R^2 = 0.78$ (EC1 and CHL) and 0.71 (EC2 and CHL) for the full dataset and 0.87 (EC1 and CHL) and 0.84 (EC2 and CHL) for a month long dataset.

3.3.2. Statistical comparison between fitted baseline and output from auxiliary electrode (AE) from SNAQ Heathrow deployment

Fig. 13 (a) shows that fitted baseline (this work) tracks the auxiliary electrode 2 (AE) from the NO and CO of electrochemical sensor node (S47), although there is an offset difference for the CO data which is an artefact of the way the method describe here works. This is not a problem with the overall data processing as the baseline-temperature corrected data can be rebased to daily background CO mixing ratios. We also noticed from this result that the CO sensor show relatively low baseline-temperature dependence compared to NO as stated in Section 2.4.

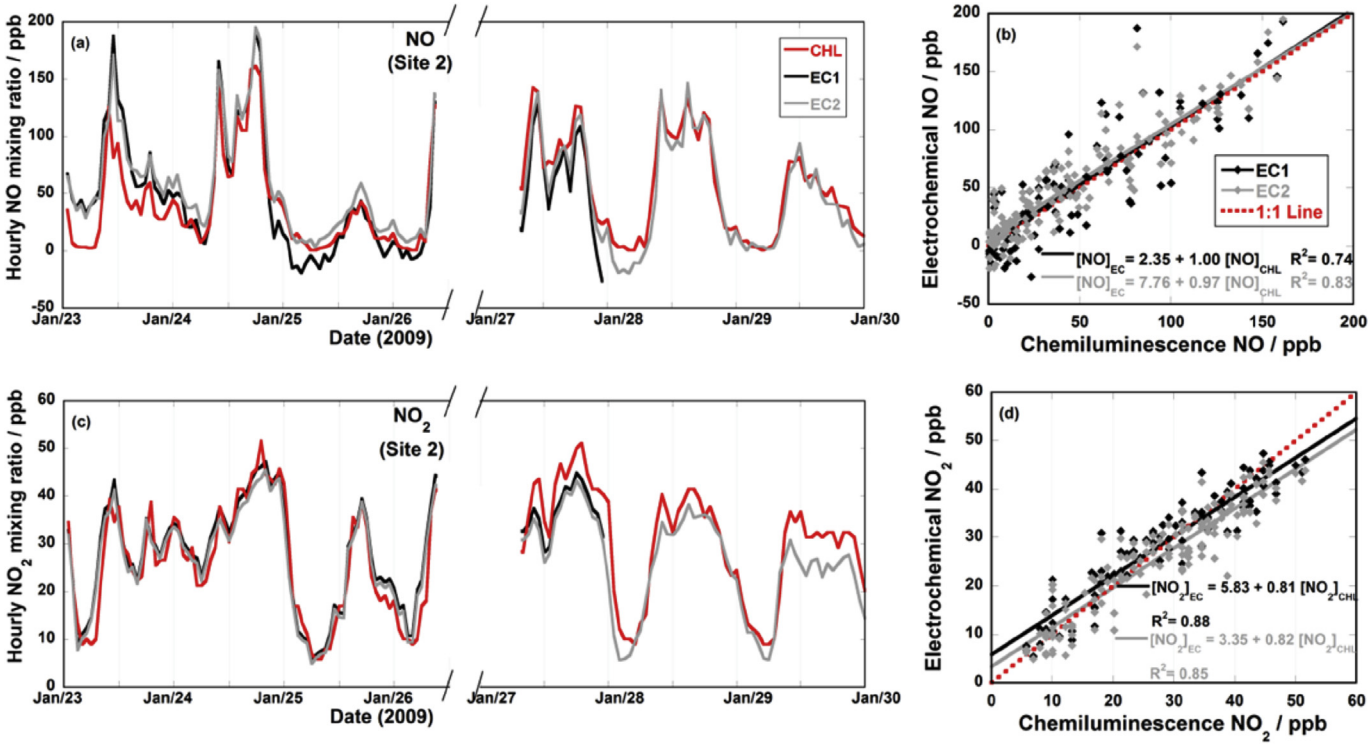

Fig. 10. Time series and relationship plots of hourly NO and NO_2 measurements using a pair of electrochemical sensor node (EC1 and EC2) and chemiluminescence instrument (CHL) at site 2, Regent Street (23–29 January 2009).

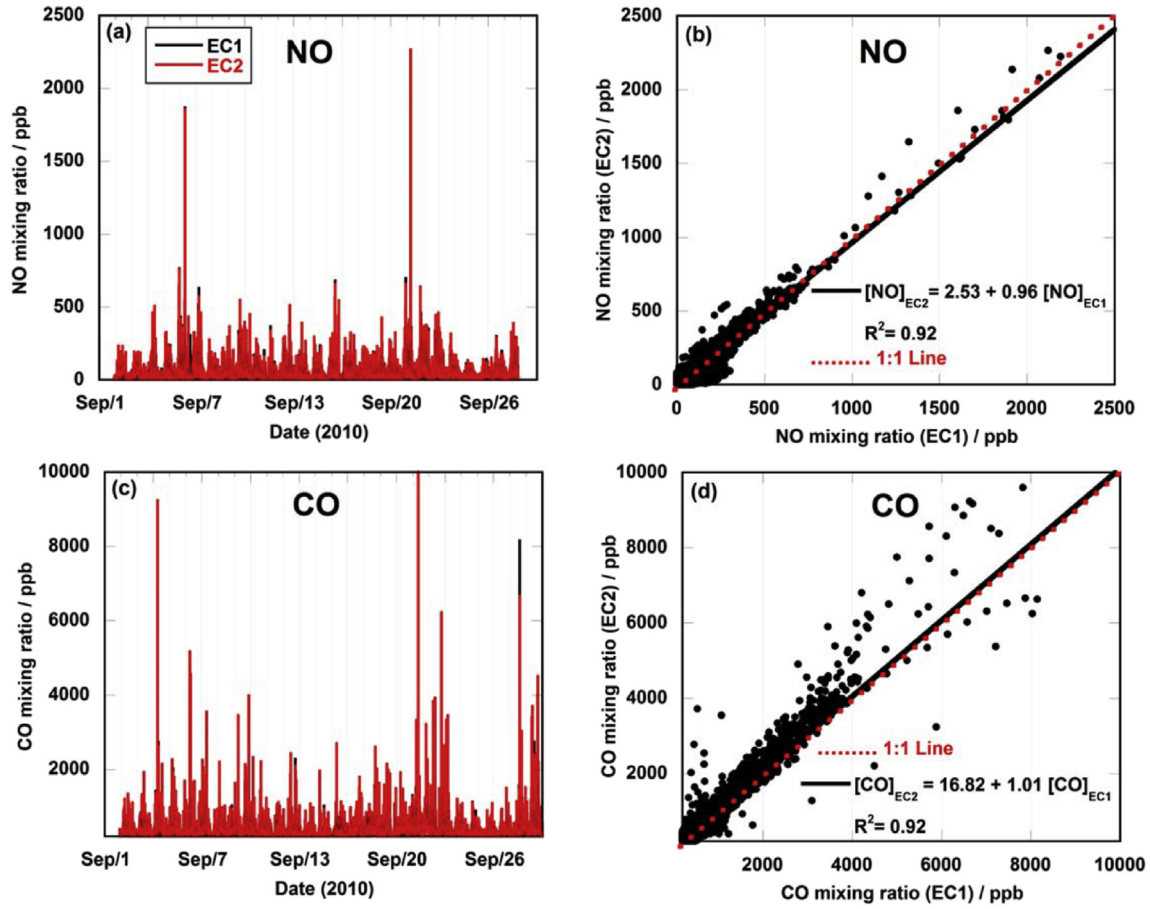

Fig. 11. Time series of 5 s, baseline-temperature corrected NO and CO mixing ratios measured by EC1 and EC2 at Gonville Place (2–28 September 2010) (a) and (c), and scatter plots showing relationship between the two sensors (b) and (d).

Table 2
Statistics associated with 5 s, baseline-temperature corrected NO and CO measurements from two electrochemical sensor nodes (EC1 & EC2) for the period 2–28 September 2010 at (site 1), Gonville Place.

Sensor (s)	Mean/ppb	SD/ppb	Max/ppb	Mean/ppb	SD/ppb	Max/ppb
	NO			CO		
EC1	34	41	2200	290	180	9400
EC2	35	41	2300	300	190	12,000

Table 3
Relationship coefficients between electrochemical sensor nodes (EC1 & EC2) and the chemiluminescence instrument for hourly uncorrected and temperature-corrected NO data over the duration of the deployment.

Species	First-order Equation	R^2
Uncorrected NO	$NO_{(EC1)} = (1.40 \times NO_{(CHL)}) + 251.31$	0.02
	$NO_{(EC2)} = (1.64 \times NO_{(CHL)}) + 273.88$	0.02
Temperature-corrected NO	$NO_{(EC1)} = (0.94 \times NO_{(CHL)}) - 0.94$	0.78
	$NO_{(EC2)} = (0.93 \times NO_{(CHL)}) + 3.23$	0.71

The residual between the baseline data show a normal distribution about zero (Fig. 13b) with RMSE < 2 ppb for NO and <10 ppb for CO (Table 4). There is good agreement between the fitted-baseline and AE data (italics Table 4) with $R^2 = 0.99$ with a gradient of 1.08 ± 0.0002 for NO and with $R^2 = 0.73$ with a gradient of 0.73 ± 0.02 as seen in. This shows that the correction method described in this work can reproduce the effects of temperature related anomalies on the baselines of electrochemical sensors. The fewer data points (N) recorded in some sensor nodes (Table 4) is as a result of failure during data transmission via GPRS network during the SNAQ Heathrow deployment. While the results summarized in Table 4 show some very good agreement ($R^2 > 0.9$) in NO, the CO data show slight agreement ($0.5 < R^2 < 0.73$). There are two possible reasons for this; firstly the CO temperature baseline shows very little temperature dependence and the new 4 electrode may not be adequately capturing this very subtle temperature change. In any case, the RMSE values of the residual in Table 4 of CO although on average 4 times that of NO, is still relatively very small compared to the absolute ambient values recorded for this species which are in hundreds and sometimes thousands of ppb.

3.4. Performance of baseline-temperature corrected electrochemical sensors

In order to evaluate the overall performance of the electrochemical sensor nodes in measuring ambient NO relative to the CHL, the differences in measured NO between the temperature-corrected pair of electrochemical sensors and CHL were calculated. In addition, the differences in NO measurements between

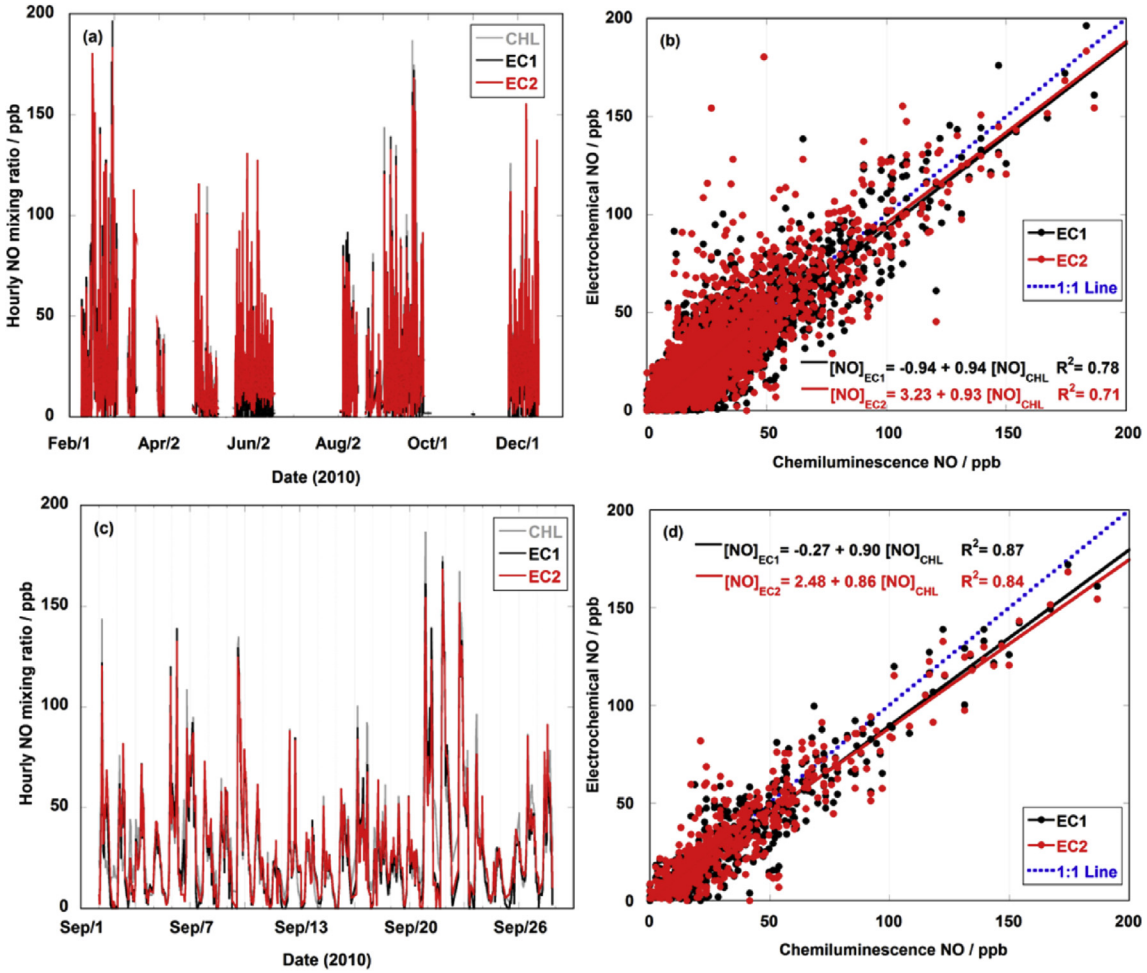

Fig. 12. Time series and regression plots of baseline-temperature corrected NO measurements from a pair of electrochemical sensor nodes and a chemiluminescence instrument for (a) hourly mean NO mixing ratios measured over the entire duration of the deployment (February–December 2010) at the AURN site in Gonville Place, Cambridge and (b) hourly means measured over one month of the same deployment (2–28 September 2010).

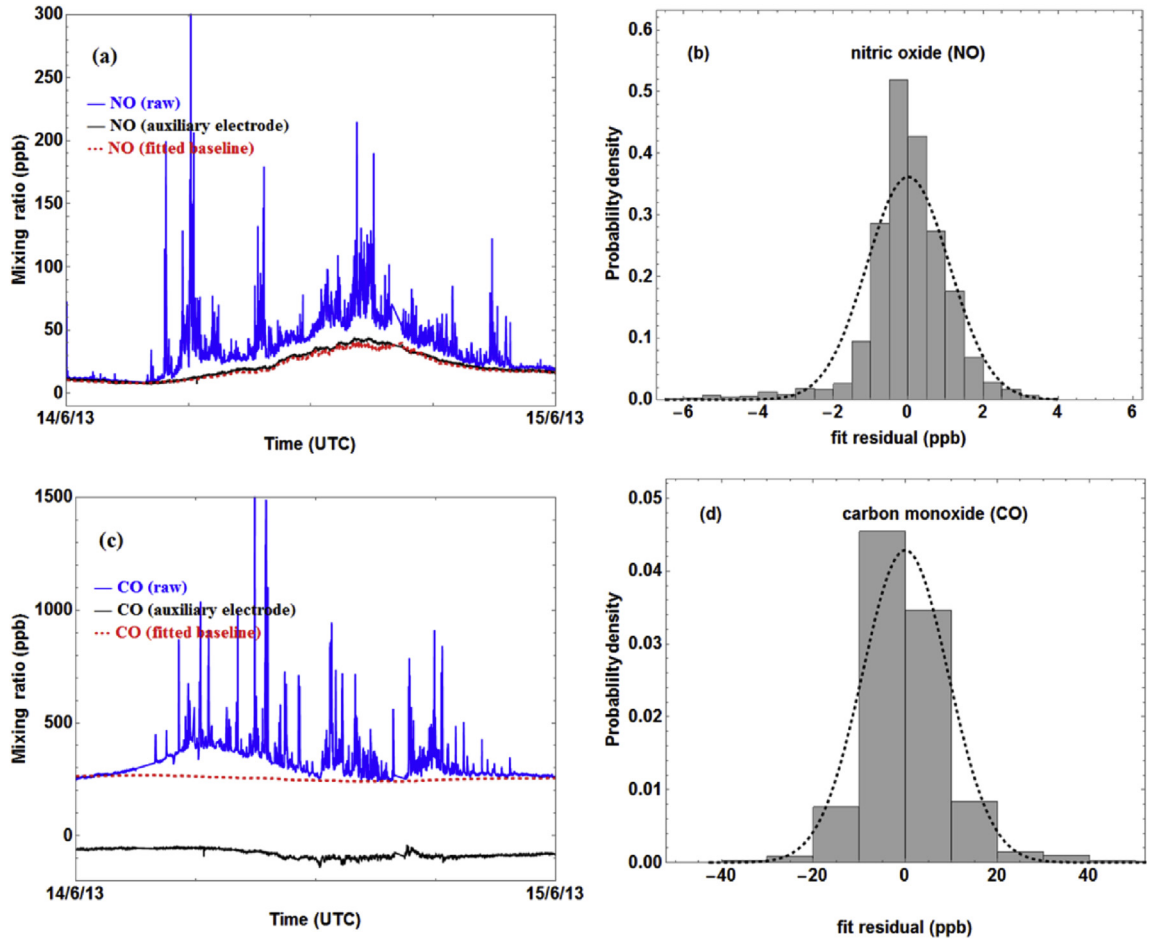

Fig. 13. Time series plot showing 24 h data (14 June 2013) of raw measurements from node S47, fitted baseline and auxiliary electrode 2 (AE) output for NO (a) and CO (c) and the corresponding probability density plots of the bias between AE and the fitted baselines for NO (b) and CO (d).

Table 4
Summary of the regression coefficients including the standard errors (se) between fitted baselines and AE output for five CO and NO EC sensor nodes at LHR on 14 June 2013. Statistics of the regression plot of S47 shown in Fig. 13 are shown here in italics. N represents the number of data points for each sensor node.

Node	NO			CO			Number of data
	R^2	gradient ± se	RMSE (ppb)	R^2	gradient ± se	RMSE (ppb)	
S09	0.99	0.79 ± 0.002	2.23	0.50	0.35 ± 0.010	7.30	2357
S28	0.99	0.80 ± 0.001	0.78	0.47	0.34 ± 0.006	9.77	3580
S42	0.98	0.76 ± 0.002	1.69	0.50	0.56 ± 0.011	6.74	2808
S47	*0.99*	*1.08 ± 0.002*	*1.10*	*0.73*	*1.83 ± 0.02*	*9.30*	*3875*
S52	0.97	0.76 ± 0.002	1.84	0.60	0.42 ± 0.005	4.95	4013

EC1 and EC2 were also determined with a summary of the statistics generated from the data gathered between the 2nd and 28th of September 2010 (presented in Table 5). The differences between the two instruments (EC1 and CHL as well as EC2 and CHL) range between −38 and + 61 ppb. Although this appears to be a large variation, majority of the values lie between ±5 ppb for EC1 and CHL and 0 to +5 ppb for EC2 and CHL (as shown in Fig. 14 (b)). This is similar to the difference observed between EC1 and EC2, with the modal bin of the histogram ranging between −5 and 0 ppb (Fig. 14 (b)). In addition, the mean values of the differences were calculated to be −4.0 ppb (EC1 and CHL), −2.0 ppb (EC2 and CHL) and −2.0 ppb (EC1 and EC2). The mean of the differences between the two instruments is small and therefore an indication of the suitability of baseline-temperature corrected NO electrochemical sensors for measurements of ambient NO mixing ratios over extended periods (several months).

Table 5
Statistics associated with the differences in NO measurements between a chemiluminescence instrument and the pair of baseline-temperature corrected NO electrochemical sensor (EC1 and EC2), and the difference between EC1 and EC2 for the period 2–28 September 2010 at site 1, Gonville Place.

Sensor (s)	Mean/ppb	SD/ppb	Range/ppb
EC1 - CHL	−4.0	10	−38 to 41
EC2 - CHL	−2.0	12	−47 to 61
EC1 - EC2	−2.0	5.0	−36 to 35

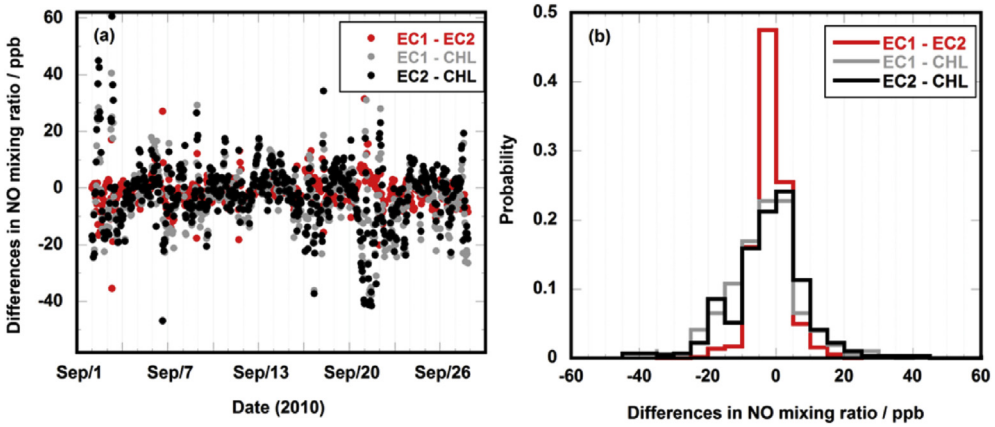

Fig. 14. Time series of the differences between hourly baseline-temperature corrected NO mixing ratios of EC1 with EC2, EC1 with CHL and EC2 with CHL (a) and histograms showing the distributions of these differences (b) at Gonville Place (2–28 September 2010).

3.5. Comparison with laboratory studies

Our aim is to develop an independent correction methodology which can be validated against reference instrument. Our approach show that while there may be an indication of a generic correction evident in similarity between the different daily correction fits using the method described in Section 2.5 (for six days shown in Fig. 15 (c)), it is not sufficient enough as there are diel variations over couple days (15 December and 16 September) that cannot be adequately represented by a single correction approach as will be the case with using the laboratory data from Alphasense (Fig. 15(a and b)). While the manufacture data may be sufficient for laboratory studies where experimental conditions can be well controlled, our results show that individual (daily) correction will give the best temperature baseline correction in real world application of these sensors evident in the results presented in the validation of the method described in this work (Section 3.4). Note the Alphasense data is of a CO AF sensor rather than NO sensor. The application notes do not have similar plots for NO sensor.

3.6. Long-term stability of baseline-temperature corrected electrochemical sensors

The NO measurements at site 1 offered the opportunity to assess the long-term stability of the temperature-corrected electrochemical sensors. The temporal change in the sensitivity (or gain) was determined by calculating the ratio of (temperature-corrected) NO measurements made using the electrochemical sensor to that from the chemiluminescence instrument for discrete periods when continuous measurements were made during the deployment. It was assumed that the chemiluminescence instrument had a stable gain as data from this instrument were ratified. Fig. 16 (a) shows the time series of the relative gain change of the NO electrochemical measurements for different periods between February and December 2010 at site 1. The slope of the trend line ($-4.25 \times 10^{-9} \pm 4.13 \times 10^{-9}$ per second) corresponds to a gain change of $-13\% \pm 13\%$ per annum. This shows that the electrochemical sensors had no statistically significant (two sided *t*-test, $p = 0.34$) drift in gain on an annual basis.

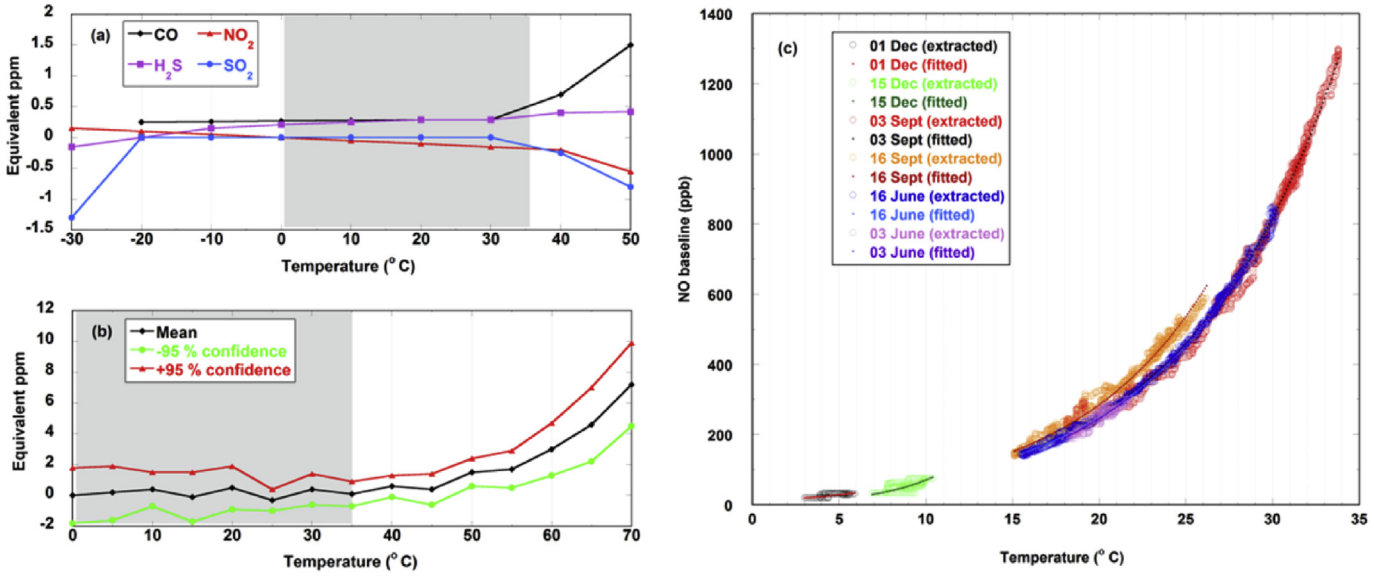

Fig. 15. Average zero current (expressed as equivalent ppm) of four sensor types with temperature (a), variability of zero current for eight CO-AF sensors from −20 to 50 °C (b), extracted (large open circles) and fitted (solid small circles) NO temperature-dependent baseline with temperature of six days including 3, 16 of June and September as well as 1, 15 December 2012 (c). Grey shades show temperature range equivalent to Fig. 15 (c). Adapted from Figs. 5 and 7, Alphasense application notes AAN110.

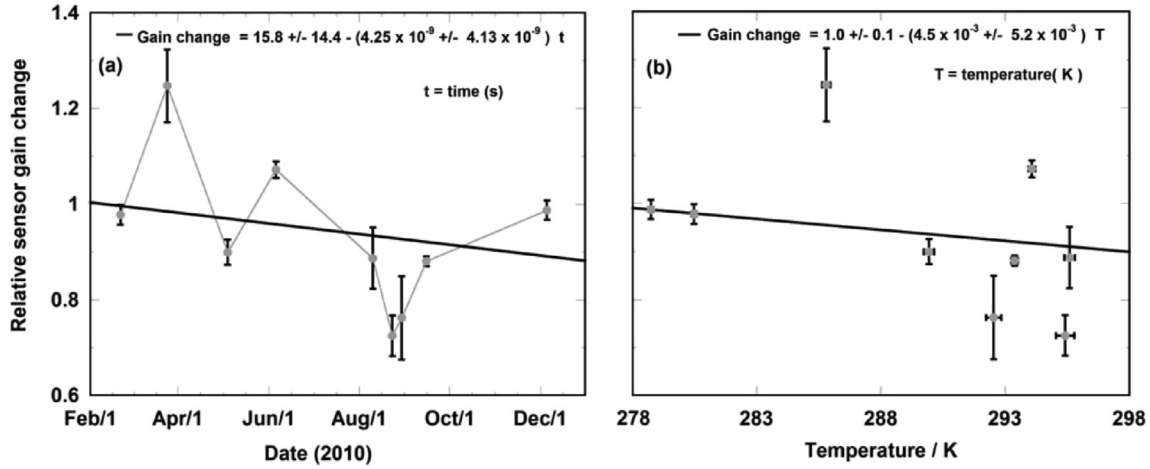

Fig. 16. Time series of the relative gain changes of NO measurements from an electrochemical sensor node, with respect to a chemiluminescence instrument, for different periods between February and December 2010 at site 1, Gonville Place (a), and a regression plot of mean temperature against relative gain changes of NO measurements from the electrochemical sensor with respect to the chemiluminescence instrument during the same period (b). The error bars represent ±1 standard error of the mean ratio estimate for each period.

The relative gain change of the NO electrochemical sensor with temperature (see Fig. 16 (b)) also demonstrates that there was no significant change in gain with temperature, as indicated by the small gradient associated with the trend line ($-4.5 \times 10^{-3} \pm 5.2 \times 10^{-3}$ per K) with p-value of 0.41. This result further validates the temperature correction methodology described in Section 2. The effect of other meteorological parameters on the long-term stability of baseline-temperature corrected NO electrochemical sensors were also evaluated using a similar analytical method to that outlined above for both time-dependent and temperature-dependent drift. A summary of the relative change in gain in relation to some meteorological parameters is presented in Table 6.

As observed for temperature, there was no noticeable change in gain with respect to relative humidity (RH). This implies that the baseline-temperature correction also accounted for the RH change as the absolute humidity does not vary much over the day as indicated in the typical strong anti-correlation often observed between temperature and RH. Similarly, results from this deployment showed that there was no significant gain change associated with pressure for the duration of the deployment. A small negative gain dependence to wind speed was observed although the source of this effect is unknown.

4. Conclusions

The deployment of electrochemical sensors under a range of ambient conditions has shown that variations in temperature result in baseline changes which may affect the sensor measurements. While the sensors perform well under temperature-controlled environments, by not taking into account the temperature effects on baseline would limit their application under ambient outdoor conditions. This work outlines a robust temperature-baseline correction methodology for electrochemical sensors thereby making these techniques more suitable for ambient air quality application.

Table 6
Regressions of the gain of baseline temperature corrected NO sensor in relation to some meteorological variables. Errors included represent ±standard error.

Variable	Gain change dependence
Ambient temperature/K	$-4.5 \times 10^{-3} \pm 5.2 \times 10^{-3}$
Pressure/hPa	$-4.4 \times 10^{-3} \pm 9.0 \times 10^{-3}$
RH/%	$-1.2 \times 10^{-3} \pm 5.2 \times 10^{-3}$
Wind speed/ms^{-1}	-0.12 ± 0.046

This correction methodology has been shown to be reproducible for the electrochemical sensors used in this study. In addition, the results presented have demonstrated that the effect of temperature on the baseline of electrochemical sensors can be successfully removed, shown by a significant improvement in the correlation of NO measurements made with electrochemical sensors to those obtained using a chemiluminescence instrument ($R^2 = 0.8$, compared to 0.02 prior to correction). Thus, the dominant environmental factor affecting the NO measurement (in this case temperature) has been accounted for. The small mean (<−4.0 ppb) of the difference between temperature-corrected hourly averaged NO electrochemical sensors and the calibrated chemiluminescence instrument signifies that the measurements from the electrochemical sensors now provide a true representation of ambient NO levels. In addition, comparison with novel four-electrode electrochemical sensors show overall good agreement between the fitted-baseline in this work and the measurements from the auxiliary (temperature-compensating) electrode for both NO ($R^2 = 0.9$), and CO ($0.5 < R^2 < 0.73$).

It has been shown that temperature-corrected electrochemical sensors do not demonstrate a statistically significant drift in gain (p-value = 0.34) on an annual basis, which makes them suitable for use for long-term studies. In addition, there was no significant change in gain due to meteorological parameters including pressure, RH and temperature following implementation of the baseline temperature correction. However, a small, negative gain change related to wind speed was observed.

Overall, for practical applications of electrochemical sensors in monitoring air quality under ambient conditions, simultaneous ambient temperature measurements are required. By implementing the temperature-correction methodology described in this paper, electrochemical sensors may be used to provide quantitative measurements at the parts per billion volume mixing ratio level typical of ambient conditions in the urban environment. In effect, electrochemical sensors may therefore be employed as a reliable and cost-effective monitoring technique that may complement existing air quality monitoring infrastructures, providing high-resolution spatial and temporal measurements within the urban

environment with a large number of applications in atmospheric science as have been shown in recent studies involving these sensors (Mead et al., 2013). By applying the baseline-temperature correction method developed in this paper, long-term studies involving network of electrochemical sensors can be carried out with improved reliability. Although there have been developments in trying to physically quantify the baseline-temperature effects using novel four electrode systems, this approach is not always reliable therefore requiring additional statistical correction method as the one presented in this work.

Acknowledgements

The authors would like to thank Jo Dicks and Anita Lewis, Environmental Services, Cambridge City Council for facilitating the comparative studies through the provision of data from the reference instruments at the monitoring stations; Brian Jones, Digital Technology Group, University of Cambridge for providing some of the meteorology data used in this work; Vivien Bright, University of Cambridge for proof reading the manuscript. Appreciation also goes to John Saffell and Ronan Baron of Alphasense Ltd, UK. The authors would also like to thank Cambridge Commonwealth Trust & Cambridge Overseas Trust and Dorothy Hodgkin Studentship for the PhD studentship awarded to Olalekan Popoola. We will like to thank NERC for funding the SNAQ Heathrow project as well as DfT and EPSRC for funding the MESSAGE project.

References

Alphasense Application Note, AAN 110 ENVIRONMENTAL CHANGES: TEMPERATURE, PRESSURE, HUMIDITY. http://www.alphasense.com/WEB1213/wp-content/uploads/2013/07/AAN_110.pdf.

Bright, V., Bloss, W., Cai, X.M., 2011. Modelling atmospheric composition in urban street canyons. Weather 66, 106–110.

DEFRA, 2009. QA/QC Procedures for the UK Automatic Urban and Rural Air Quality Monitoring Network (AURN), 5,21.

De Vito, S., Piga, M., Martinotto, L., Di Francia, G., 2009. CO, NO2 and NOx urban Pollution monitoring with on-field calibrated electronic nose by automatic Bayesian regularization. Sens. Actuators B 143, 182e191.

DIRECTIVE 98/69/EC OF THE EUROPEAN PARLIAMENT AND OF THE COUNCIL of 13 October 1998 relating to measures to be taken against air pollution by emissions from motor vehicles and amending Council Directive 70/220/EEC Off. J. Eur. Union L350, 0001–0057.

DIRECTIVE 2009/28/EC OF THE EUROPEAN PARLIAMENT AND OF THE COUNCIL of 23 April 2009 on the promotion of the use of energy from renewable sources and amending and subsequently repealing Directives 2001/77/EC and 2003/30/EC. Off. J. Eur. Union L140, 16.

Hitchman, M.L., 1978. Measurement of Dissolved Oxygen. Wiley, New York.

Hitchman, M.L., Cade, N.J., Gibbs, T.K., Hedley, N.J.M., 1997. Study of the factors affecting mass transport in electrochemical gas sensors. Analyst 122, 1411–1417.

Mead, M.I., Popoola, O.A.M., Stewart, G.B., Landshoff, P., Calleja, M., Hayes, M., Baldovi, J.J., Hodgson, T., McLeod, M., Dicks, J., Lewis, A., Cohen, J., Baron, R., Saffell, J., Jones, R.L., 2013. The use of electrochemical sensors for monitoring urban air quality in low-cost, high-density networks. Atmos. Environ. 70, 186–203.

Popoola, O., Mead, I., Bright, V., North, R., Stewart, G., Kaye, P., Jones, R., 2013. A portable low-cost high density sensor network for air quality at London Heathrow airport. In: AGU 2013 Fall Meeting, San Francisco, California.

Stetter, J.R., Li, J., 2008. Amperometric gas sensors-A Review. Chem. Rev. 108, 352–366.